Astron. Astrophys. 265, 656–662 (1992)

ASTRONOMY AND ASTROPHYSICS

Unified NLTE model atmospheres including spherical extension and stellar winds

III. The EUV fluxes of hot massive stars and He II emission in extragalactic giant H II regions

R. Gabler[1], A. Gabler[1], R.P. Kudritzki[1,2], and R.H. Méndez[1*]

[1] Institut für Astronomie und Astrophysik der Universität München, Scheinerstr. 1, W-8000 München 80, Federal Republic of Germany

[2] Max-Planck-Institut für Astrophysik, Karl-Schwarzschild-str. 1, W-8046 Garching bei München, Federal Republic of Germany

Received May 11, accepted August 2, 1992

Abstract. We demonstrate that massive O stars sufficiently close to the Eddington limit, and with effective temperatures only slightly higher than 50 000 K, can provide enough flux shortward of 228 Å to reproduce the strength of the observed He II 4686 narrow nebular emission in the few known cases of high-excitation extragalactic H II regions. We present the results of calculations made using "unified" model atmospheres, describe the models which are able to produce the required amount of He^+ ionizing photons, and show their predicted stellar H and He optical line profiles. The spectral characteristics of these models are similar to those observed in stars classified as extreme Of supergiants or "slash" stars. We conclude that the detection of a Wolf-Rayet spectrum (broad emissions) within a high-excitation H II region (characterized by showing narrow 4686 emission) may not necessarily be a definitive proof that a WR star is the source of He^+ ionizing photons.

Key words: stellar atmospheres – early-type supergiant stars – high-excitation H II regions

1. Introduction

For the differential study of giant extragalactic H II regions (GEHRs) in normal and starburst galaxies, the investigation of their stellar content has become a crucial point. From the absence of He II emission lines in the recombination spectra of GEHRs, it is normally concluded that the effective temperatures of the ionizing stars are well below 60 000 K (Campbell 1988; Vilchez & Pagel 1988), which is in agreement with the temperatures of the most massive and hottest main sequence stars we know in our Galaxy (Kudritzki & Hummer 1986, 1990; Kudritzki et al. 1991).

On the other hand, a few cases of high-excitation H II regions exist. The earlier detections were ambiguous, because the moderate resolution of the one-dimensional detectors used at that time did not permit to distinguish between nebular and stellar emission (Bergeron 1977). More recently, however, using the techniques of long-slit 2D-detector spectroscopy, it has become clear that indeed a few extragalactic H II regions show definite nebular He II 4686 emission (Pakull & Angebaut 1986; Stasinska et al. 1986; Pakull & Motch 1989; Garnett et al. 1991).

This definite detection of extended nebular He II 4686 emission has led to question about the physical nature of the ionizing stellar sources (see Pakull & Motch 1989; Garnett et al. 1991 for a detailed discussion). Hot Wolf-Rayet stars, massive X-ray binaries or radiative shocks in the H II regions are considered to be possible explanations, while normal, massive O stars are ruled out mainly because, given the ionizing EUV flux predicted by NLTE model atmospheres, stars hotter than 60 000 K would be required, which are unlikely to exist.

The purpose of this paper is to demonstrate that the automatic rejection of massive O stars is not justified. Extending our previous calculations of unified model atmospheres for massive stars (Gabler et al. 1989 (Paper I); Kudritzki et al. 1991) to objects very close to the Eddington limit, we have found that extreme supergiants with effective temperatures only slightly higher than 50 000 K can provide enough flux shortward of 228 Å to reproduce the strength of the observed He II 4686 emission.

In Sect. 2 we present a grid of ionizing fluxes obtained from unified model atmospheres for massive stars. We show that, for objects hotter than 50 000 K, the flux of He^+ ionizing photons depends crucially on the distance from the Eddington limit. In Sects. 3 and 4 we describe the models which are able to reproduce the observed ratio of nebular He II 4686 to H_β line strengths. For the candidate models we show calculated stellar line profiles of optical H and He lines. Section 5 contains a final discussion.

2. The calculation of ionizing fluxes

As demonstrated in Papers I and II (Gabler et al. 1991), the influence of stellar wind mass outflow is extremely important for the formation of the stellar continuum shortward of the He II ionization edge at 228 Å. As a result, the number of He^+ ionizing photons can be raised by a factor up to 1000 relative to

Send offprint requests to: R. Gabler

*Member of the Carrera del Investigador Cientifico, CONICET, Argentina

hydrostatic, plane-parallel NLTE model atmospheres that ignore the stellar winds. In Paper II we have investigated the importance of these stellar wind effects on the ionization of planetary nebulae. Here we want to study the He^+ ionization of H II regions by massive stars.

For that purpose we have calculated a grid of NLTE unified model atmospheres with 35 000 K $< T_{\rm eff} <$ 51 000 K and radii and surface gravities representative of massive main sequence stars (V) and supergiants (I). The stellar parameters are given in Table 1, and correspond roughly to the results of recent quantitative NLTE spectral analyses of Galactic O-stars (Herrero et al. 1992; Kudritzki et al. 1992). Temperatures are given in thousands of K, Γ is the ratio of stellar to Eddington luminosity, and L.C. indicates the luminosity class.

Note that a discrepancy has recently been found between O-star masses derived from spectroscopy ("spectroscopic masses") and from evolutionary tracks using stellar luminosities ("evolutionary masses"). For a discussion of this discrepancy we refer the reader to Groenewegen et al. (1989), Herrero et al. (1992) and Kudritzki et al. (1992).

Table 1. The grid of unified model atmospheres for the He^+ ionization problem

$T_{\rm eff}$	log g	$R/R_\odot$	$M/M_\odot$	Γ	L.C.	$Z_{\rm HeII} - Z_{\rm H}$
35	4.0	7.5	20.5	0.09	V	-4.42
35	3.2	36.0	75.0	0.58	I	-4.39
40	4.0	10.0	36.5	0.15	V	-3.36
40	3.4	28.0	71.9	0.62	I	-3.76
45	4.0	12.0	52.6	0.25	V	-3.29
45	3.6	19.0	52.5	0.63	I	-3.58
45	3.482	29.6	96.7	0.873	I*	-3.85
51	3.9	20.0	116.0	0.52	V	-3.52
51	3.75	23.0	108.6	0.74	I	-2.56
51	3.7	23.0	96.8	0.872	I*	-1.53
55	3.831	19.8	96.8	0.873	I*	-1.67

As described in papers I and II, the unified models make no artificial separation between a hydrostatic photosphere and a supersonically expanding stellar wind. Instead, a detailed radiatively driven wind code, giving the density structure and velocity field along the whole (sub- and supersonic) atmosphere, is combined with a NLTE model atmosphere code for spherical geometry, which gives the temperature structure. In this way, the whole atmospheric structure can, in principle, be described self-consistently as a function of three basic stellar parameters: $T_{\rm eff}$, log g, and the stellar radius at which $T_{\rm eff}$ and log g are given (this stellar radius fixes the stellar luminosity and mass), plus the chemical composition. For the present calculations we have included only H and He. The possible effects of metal line blanketing are briefly discussed at the end of this section.

In order to describe the production of ionizing photons by the unified models, we use the logarithmic Zanstra ratios, $Z_{\rm HeII}$ and $Z_{\rm H}$, defined in the following way:

$$\log\left(\frac{\text{number of ionizing photons (cm}^{-2}\text{ s}^{-1})}{\text{stellar continuum flux at 5480Å (erg cm}^{-2}\text{ s}^{-1}\text{ Hz}^{-1})}\right).$$

The following are expressions for the observed H and He II logarithmic Zanstra ratios:

$$Z_{\rm H} = 30.825 + \log F_\beta + 0.4\ V + 0.13\ c + \log\left(\frac{\alpha_B({\rm H})}{\alpha({\rm H}_\beta)}\right) \quad (1)$$

$$Z_{\rm HeII} = 30.809 + \log F_{4686} + 0.4\ V + 0.17\ c + \log\left(\frac{\alpha_B({\rm He}^+)}{\alpha(4686)}\right) \quad (2)$$

where the F's are observed nebular fluxes in erg cm^{-2} s^{-1}, V is the apparent visual magnitude of the exciting star, c is the logarithmic extinction at H_β, and the α's are recombination coefficients, taken from Brocklehurst (1971) and Osterbrock (1974).

The difference $Z_{\rm HeII} - Z_{\rm H}$ gives the logarithm of the ratio of the number of He^+ ionizing photons to the number of H ionizing photons. This ratio is frequently called $Q(He^+)/Q(H^0)$. From Eqs. (1) and (2) we obtain the logarithm of $Q(He^+)/Q(H^0)$ as a function of observable quantities:

$$Z_{\rm HeII} - Z_{\rm H} = \log\left(\frac{F_{4686}}{F_\beta}\right) + 0.04\ c - 0.016 + \log\left(\frac{\alpha_B({\rm He}^+)\ \alpha({\rm H}_\beta)}{\alpha(4686)\ \alpha_B({\rm H})}\right) \quad (3)$$

Garnett et al. (1991) have reported values of $Z_{\rm HeII} - Z_{\rm H}$ as high as -1.57 in extragalactic H II regions. Notice that these values can be directly compared with model calculations only if we assume that no ionizing photons are leaking from the H II region. If the nebula absorbs all the He^+ ionizing photons, but some H ionizing photons are able to escape (a common situation in planetary nebulae, see e.g. Méndez et al. 1992), then the measured H_β flux is lower, and the observed value of $Z_{\rm HeII} - Z_{\rm H}$ is misleadingly high.

In Table 1 we have listed the computed values of $Z_{\rm HeII} - Z_{\rm H}$ for all our models of the luminosity sequences I and V. In Fig. 1 these values are compared with those obtained from plane-parallel, hydrostatic non-LTE models, as well as with the observed range of $Z_{\rm HeII} - Z_{\rm H}$ in extragalactic H II regions, as discussed by Garnett et al. (1991). Obviously, the strong increase of flux in the He II continuum of the unified models is still not sufficient to explain the observed ratio of nebular He II 4686 to H_β emission, as already reported by Garnett et al. (1991).

However, from our previous work we expect that, near the Eddington limit, small changes in surface gravity may lead to substantial changes in the stellar wind. We have, therefore, calculated another supergiant model with $T_{\rm eff}$ = 51 000 K and with the same radius as model I, but with a marginally (0.05 dex) reduced gravity. We call this model "extreme" or "I*" supergiant, and note that from the viewpoint of photospheric NLTE diagnostics it would be difficult to detect the difference in gravity between I and I*.

From Table 1 and Fig. 1 we see that this small change in gravity (or mass) is sufficient to increase the He II continuum flux by one order of magnitude. As will be explained in Sect. 3, this is a direct consequence of the fact that the stellar wind density increases strongly when coming closer to the Eddington limit. Thus, the distance from the Eddington limit is crucial for the formation of the He II continuum, at least at this effective temperature.

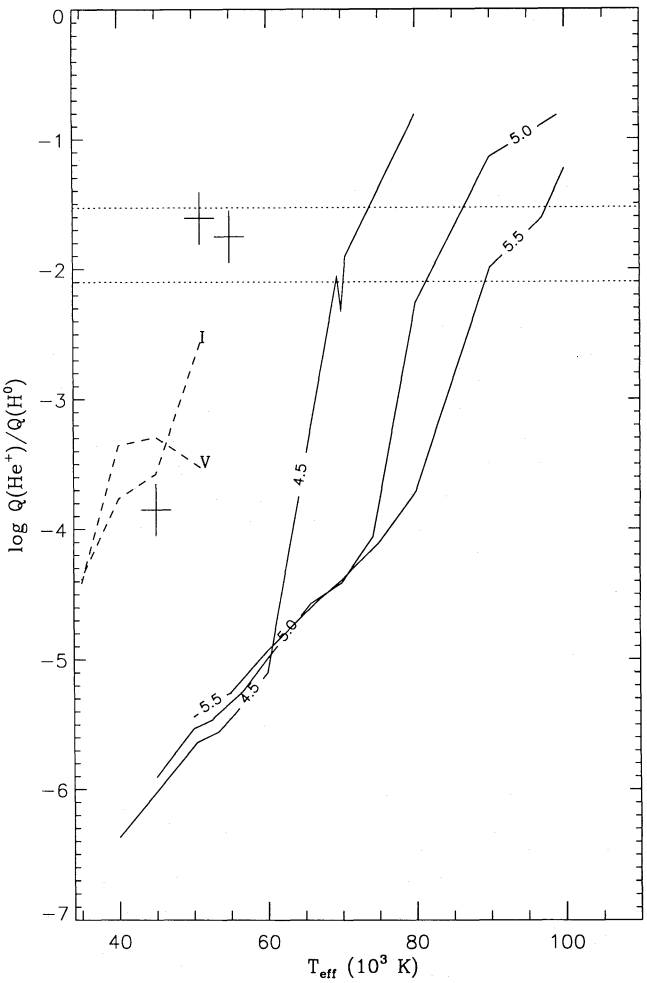

Fig. 1. The ratio of the number of He^+ ionizing photons to the number of H ionizing photons, plotted as a function of stellar effective temperature. The full lines are ratios obtained from plane-parallel, hydrostatic NLTE models with log g = 4.5, 5.0 and 5.5. The dashed lines are ratios obtained from the V and I unified models listed in Table 1. The plus signs are ratios obtained from the I* unified models in Table 1. The horizontal dotted lines indicate the range of observed ratios in high-excitation extragalactic H II regions, as discussed by Garnett et al. (1991)

To investigate the temperature dependence of this effect, we have calculated two additional models (also labeled I* in Table 1) with the same luminosity and distance from the Eddington limit, but $T_{\rm eff}$ = 45 000 K and 55 000 K, respectively. The hotter model shows again a strongly increased He II continuum flux, whereas a decrease is found in the cooler case. In Sect. 3 we will discuss this behaviour.

We conclude that the two hottest I* models of Table 1, with $T_{\rm eff}$ well below 60 000 K, are able to produce the required amount of He^+ ionizing photons, even if we assume that no H ionizing photons are escaping.

Notice that our models do not include the effects of metal line blanketing. This means, that we do not take into account the influence of the blanketing on the formation of the He II resonance line at 303 Å, which is of importance for the formation of the He II continuum (see Paper I and II). Unfortunately we cannot estimate how important this effect is for the calculation of the number of He^+ ionizing photons, because at the present time it is not possible to calculate metal line blanketing reliably for spherical models with mass outflow. Almost all reported cases of high excitation H II regions are associated with low metallicity (see Sect. 5); we are assuming that the blanketing effect, at least in such cases, does not produce qualitative changes in our results.

3. A comparison of two very similar models

The model sequence at $T_{\rm eff}$ = 51 000 K demonstrates that, close to the Eddington limit, nearly identical stars may produce widely different amounts of He^+ ionizing photons, if they are hot enough. A similar situation is known to exist among the central stars of planetary nebulae: low-excitation PN show a very good correlation between nebular excitation class and stellar $T_{\rm eff}$ (Pauldrach et al. 1988; Kaler & Jacoby 1991; Méndez et al. 1992), but the correlation is lost as soon as He II 4686 becomes visible in the nebular spectrum. To understand this behaviour, we compare directly the two 51 000 K models with slightly different gravities (log g = 3.70 Model A, log g = 3.75 Model B) given in Table 1.

The basic difference of model A relative to model B is its higher average wind (electron) density

$$\bar{n}_{\rm E} = \frac{1+2Y}{1+4Y}\,\frac{1}{m_{\rm H}}\,\frac{\dot{M}}{4\pi R^2 v_\infty} \tag{4}$$

and its lower effective gravity

$$g_{\rm eff} = g(1-\Gamma) \tag{5}$$

($\dot{M}$ is the mass loss rate, v_∞ the terminal velocity, $m_{\rm H}$ the mass of a H atom and Y the He to H number fraction). The corresponding quantities are given in Table 2.

Table 2. Properties of models A and B

Quantity	model A	model B
log $g_{\rm eff}$	2.807	3.165
$\dot{M}$ ($M_\odot$/yr)	2.7 10^{-5}	1.7 10^{-5}
v_∞ (km/s)	1725	2520
$\bar{n}_{\rm E}$ (cm^{-3})	1.56 10^{11}	6.71 10^{10}
$\tau_{\rm Ross}$ at $r_{\rm sonic}$	0.63	0.28
T(K) at $r_{\rm sonic}$	44200	40660
b_1(He II) at $r_{\rm sonic}$	5.2 10^{-3}	1.4 10^{-2}

This difference has important consequences on the atmospheric structure and on the observational quantities (see also Sect. 4).

The difference in wind density leads to a different optical thickness of the stellar wind envelope around the photosphere. Adopting a usual "β-velocity law" $v(r) = v_\infty(1-(a/r))^\beta$, where a is a little smaller than unity (ensuring that $v(1) = v_{\rm sonic}$), and $\beta \sim 0.75$ as a suitable approximation for the numerical velocity field, and using the equation of continuity, the Rosseland (=Thompson) optical depth at the sonic point can be estimated as

$$\tau_{\rm Ross}(r = r_{\rm sonic}) \sim 4\,\bar{n}_{\rm E}\,\sigma_{\rm E}\,R_\star \tag{6}$$

which yields 0.66 for model A and 0.28 for model B, in good agreement with the numerical values in Table 2 ($\sigma_{\rm E}$ is the electron scattering coefficient).

The higher optical thickness of the surrounding wind yields a higher local electron temperature at the sonic point for model

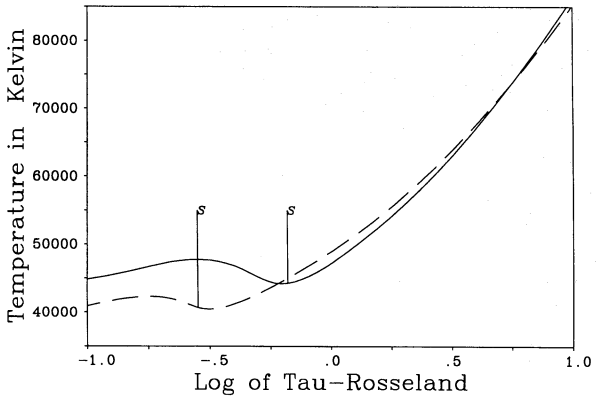

Fig. 2. Temperature structure of models A (solid) and B (dashed). The location of the sonic point is indicated by the vertical bar

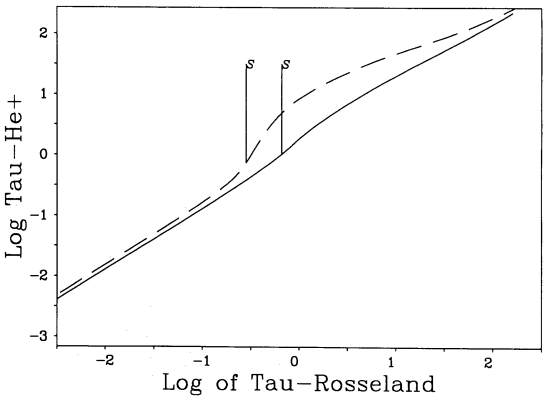

Fig. 4. Optical thickness at the He II edge as a function of log τ_{Ross} for models A (solid) and B (dashed). The sonic points are indicated

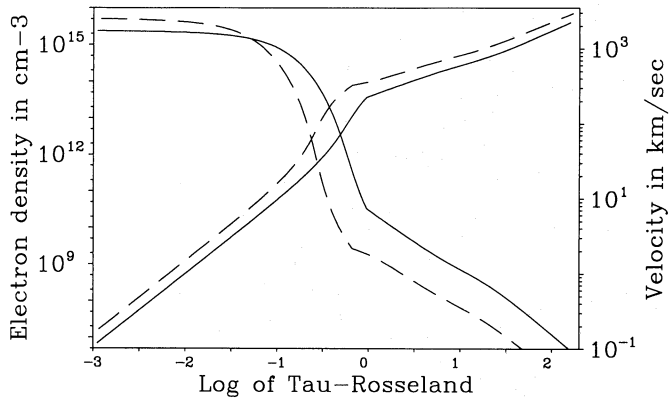

Fig. 3. Electron density (decreasing towards left) and velocity structure (increasing towards left) of models A (solid) and B (dashed)

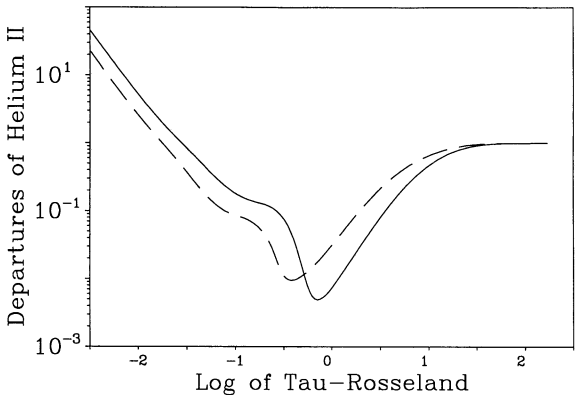

Fig. 5. Departure coefficient b_1 of models A and B

A (see Table 2 and Fig. 2). Since $h\nu/kT$ is much larger than unity for the frequencies in the He II continuum, this difference in temperature is crucial for the emission coefficient and the ionization process.

Figure 2 shows the temperature structure of the outer photosphere and the transition to the stellar wind region. The temperature minima coincide with the sonic point, where the hydrogen lines and also the stronger continua start to become optically thin, which causes the increase in temperature in both models (see Paper I and references therein).

The electron density of model A as a function of τ_{Ross} is always smaller than in model B (see Fig. 3). Above the sonic point this is a consequence of the higher mass loss rate (see Paper I). Below the sonic point, where the density follows the hydrostatic equation, this is caused by the lower value of g_{eff}. Since the He II ground-state bound-free opacity is proportional to n_{E}^2, the lower n_{E} of model A has important consequences for the NLTE radiative transfer. Figure 4 shows the optical thickness at the He II ionization edge, which is much lower in model A than in model B. $\tau_\nu \sim 1$ is reached in both models in the region around the sonic point.

Figure 5 displays the departure coefficient of the He II ground state. Around the sonic points, the typical minima, as discussed in Papers I and II, are obtained. However, in model A, b_1 at the sonic point is significantly smaller than in model B (see Table 2). This is a direct consequence of the lower electron density and the correspondingly lower thermalization of the radiation field.

Figure 6 shows the thermalization parameter λ_ν (see Husfeld et al. 1984), defined as

$$\lambda_\nu = \frac{\kappa_\nu}{\kappa_\nu + n_{\text{E}}\sigma_{\text{E}}} \tag{7}$$

at the He II edge (κ_ν is the ground-state bound-free opacity). Note that λ_ν is proportional to ν^{-3} for frequencies larger than that of the edge. λ_ν is significantly smaller in model A. For the radiative transfer, this means that the difference between the true absorption source function and the mean intensity is larger in model A. This difference can be expressed by the net radiative ionization probability, defined as

$$\widetilde{R_{1k}} = (n_1 R_{1k} - n_{\text{HeIII}} R_{k1})/n_1 \tag{8}$$

where n_1 is the He II ground-state occupation number, n_{HeIII} is the He III population density, and R_{1k}, R_{k1} are the radiative ionization and recombination probabilities. Figure 7 demonstrates how different is $\widetilde{R_{1k}}$ in models A and B, as a result of the significantly different thermalization. The rather large positive values of $\widetilde{R_{1k}}$ are a result of the temperature gradient and the correspondingly large variation of $\exp(-h\nu/kT)$ in the He II continuum. In consequence, the He II ionization is increased and ground-state

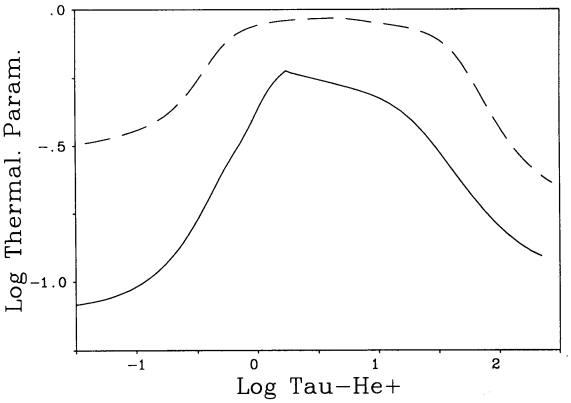

Fig. 6. Thermalization parameter λ_ν as a function of optical thickness at the frequency of the He II edge, for models A (solid) and B (dashed)

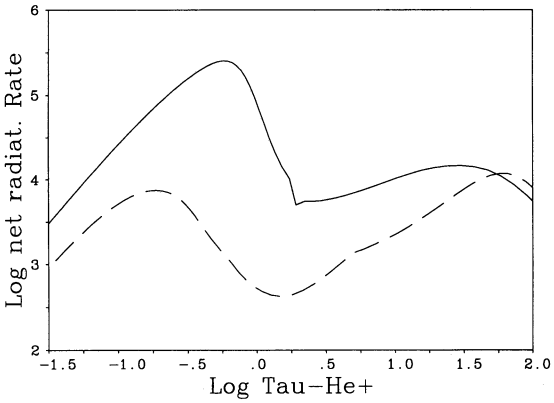

Fig. 7. Net radiative ionization probability as a function of optical thickness at the frequency of the He II edge, for models A (solid) and B (dashed)

departure coefficients smaller than unity are encountered even in deeper layers, where the influence of the line transitions is negligible. Around the sonic point, where the line effects, as discussed in Paper I, become important, the much higher value of R_{1k} in model A causes additional ionization and thus a further decrease of b_1.

From the Eddington-Barbier relation (see Husfeld et al. 1984) we know that the emergent flux is proportional to the thermal source function $S_\nu^{\rm true} = B_\nu/b_1$ at the thermalization depth $\tau_\nu^{\rm therm} = (3\lambda_\nu)^{-1/2}$:

$$H_\nu \sim (B_\nu/b_1)_{\tau_\nu^{\rm therm}} \tag{9}$$

Inspection of Figs. 6 and 4 shows that thermalization at the edge frequency occurs roughly at the sonic point. Inserting the numbers from Table 2 for T and b_1, we obtain for the ratio of emergent He II edge fluxes of models A and B:

$$\frac{H_\nu(A)}{H_\nu(B)} \sim \frac{B_\nu(A)}{B_\nu(B)}\frac{b_1(B)}{b_1(A)} \sim 9.3 \tag{10}$$

This explains why model A produces many more He II ionizing photons than model B.

4. The predicted spectrum of the I* "extreme supergiants"

The calculation of the emergent stellar H and He line profiles was performed in the same way as described in Paper I, Sect. 2.4. Figure 8 shows the predicted absorption and emission profiles of the main stellar diagnostic lines: H_α, H_β, H_γ, He II 4200, 4541 and He II 4686, for the I supergiant and for the extreme I* supergiant, (log g = 3.75 and 3.70, respectively), both having $T_{\rm eff}$ = 51 000K. He I lines are predicted to be very weak in both cases.

The I supergiant shows a predicted spectrum very similar to that of HD 93129A, as described by Simon et al. (1983). Indeed, the atmospheric parameters determined for HD 93129A by Kudritzki et al. (1992) are almost exactly those of model B: $T_{\rm eff}$ = 50 500 K and log g = 3.75).

Consider now model A: as expected from the discussion in Sect. 3, the wind effects are stronger. H_α and H_β show well-developed P Cygni profiles, but H_γ, although noticeably distorted, remains in absorption. He II 4541 is also in absorption, and is blueshifted by about 30 Km/s. He II 4686 shows a strong emission, with FWHM=12 Å, and an equivalent width of 17 Å.

An object with such spectral characteristics would be classified as an extreme case of Of supergiant, perhaps an Of/WN or "slash" star, as defined by Walborn (1982) and discussed by Conti & Bohannan (1989) and by Bohannan (1990, see in particular his Fig. 3). Since just a handful of these "slash" stars are currently known, there is a good chance that none of them in our Galaxy is hot enough to produce substantial He^+ ionization.

5. Discussion

High-excitation H II regions associated with massive stars are not frequent, and therefore, in order to explain them, we need a rather uncommon phenomenon. We believe that the "extreme supergiants" we introduced above are a plausible alternative to hot Wolf-Rayet stars.

In the case of more distant galaxies, the detection of a Wolf-Rayet spectrum (see a recent catalog and discussion of "WR galaxies" in Conti 1991) within a high-excitation H II region (characterized by the presence of *narrow* nebular 4686 emission) may not necessarily be a definitive proof that a Wolf-Rayet star is the source of He^+ ionizing photons, because it may be difficult to rule out the presence of other He^+ ionizing sources, with less spectacular spectra, like the extreme supergiants we described above. A convincing proof would be the identification of spectral WR features uniquely associated with very high temperatures, like very strong O VI emissions, as in the case of IC 1613 (Garnett et al. 1991).

An interesting observational fact is that almost all reported cases of high-excitation H II regions are associated with low-metallicity galaxies: the Magellanic Clouds and IC 1613, an irregular galaxy with Z=0.002 (Hodge 1989). The only counterexample is the bubble G2.4+1.4 in our Galaxy, excited by a WO star (Dopita et al. 1990).

This information about metallicity is potentially useful, but it would be dangerous to extract evolutionary conclusions before unambiguously clarifying what is the actual stellar content within high-excitation H II regions.

In summary, the purpose of this paper is neither to disprove the existence of Wolf-Rayet stars within high-excitation H II regions (which is well documented) nor to challenge the suggestion that very hot Wolf-Rayet stars or X-ray binaries may be the He^+ ionizing sources. Our purpose is rather to sound a cautionary

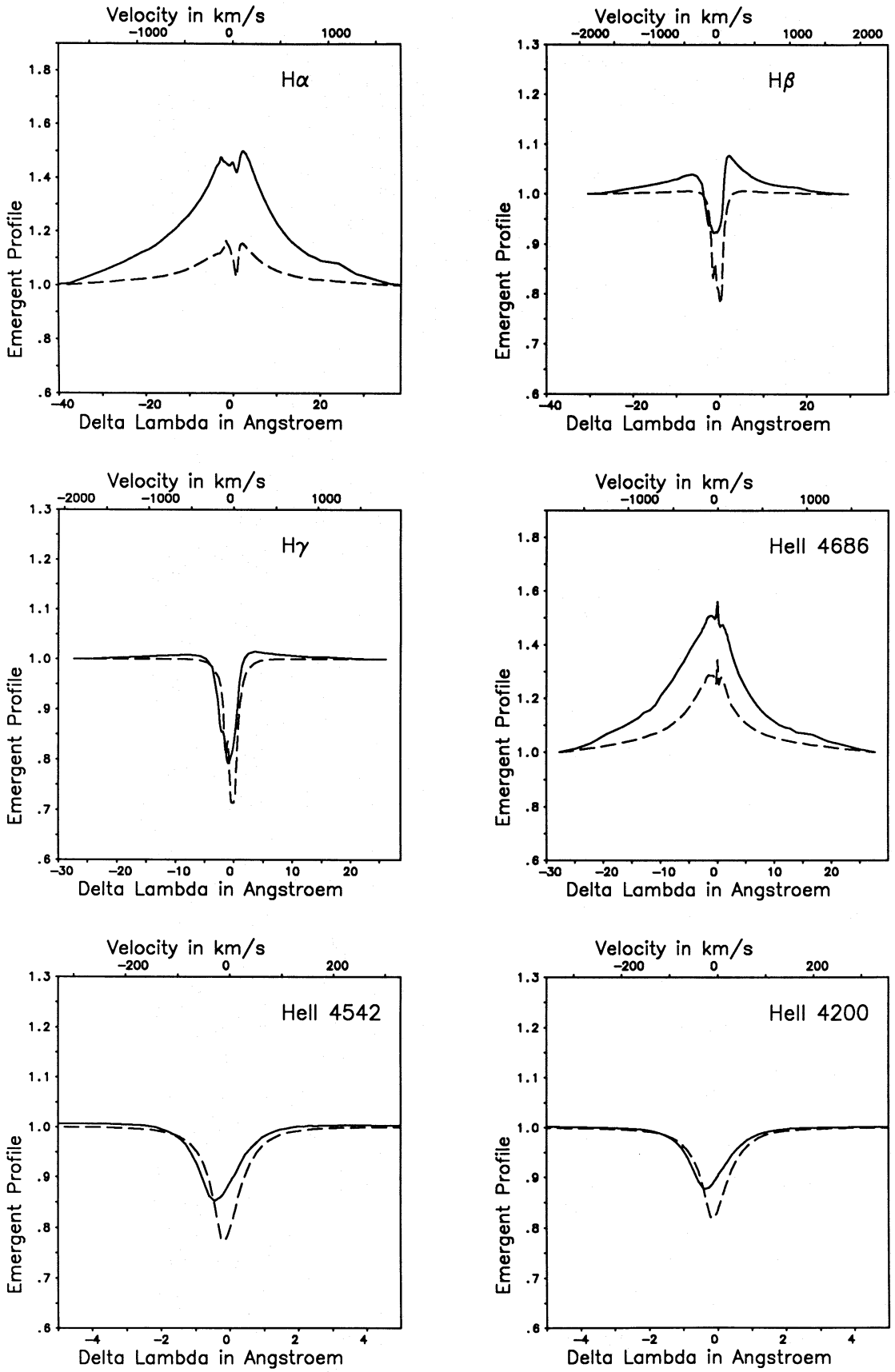

Fig. 8. Predicted H and He II absorption and emission lines for model A (log g = 3.70, solid) and B (log g = 3.75, dashed)

note: we have found an additional way of explaining the existence of H II regions with strong He II emission around massive stars, and this reinforces a warning already stated by Garnett et al. (1991): that it is not safe to replace the direct observation of the stellar content within an H II region by schematic nebular diagnostics if we want to extract reliable information.

Acknowledgements. This work was supported by the Deutsche Forschungsgemeinschaft through grant Ku 474/16, and by the BMFT through grant 010R9008.

References

Bergeron J., 1977, ApJ 211, 62
Bohannan B., 1990, in: Garmany C.D. (ed.) Properties of Hot Luminous Stars, Boulder-Munich Workshop; Astron. Soc. Pacific Conference Series, Vol. 7, p.39
Brocklehurst M., 1971, MNRAS 153, 471
Campbell A., 1988, ApJ 335, 644
Conti P.S., 1991, ApJ 377, 115
Conti P.S., Bohannan B., 1989, in: Davidson K. et al. (eds.) Proc. IAU Coll. 113, Physics of Luminous Blue Variables. Kluwer, Astrophys. Space Sci. Library 157, p.297
Dopita M.A., Lozinskaya T.A., McGregor P.J., Rawlings S.J., 1990, ApJ 351, 563
Dreizler S., Werner K., 1992, in: Heber U., Jeffery C.S. (eds.) The Atmospheres of Early-Type Stars. Springer, Lecture Notes in Physics 401, p.436
Gabler R., Gabler A., Kudritzki R.P., Puls J., Pauldrach A., 1989, A&A 226, 162 (Paper I)
Gabler R., Kudritzki R.P., Méndez R.H., 1991, A&A 245, 587 (Paper II)
Garnett D.R., Kennicutt R.C., Chu, Y.H., Skillman, E.D., 1991, ApJ 373, 458
Groenewegen M.A.T., Lamers H.J.G.L.M., Pauldrach A.W.A., 1989, A&A 221, 78
Herrero A., Kudritzki R.P., Vilchez J.M., Kunze D., Butler K., Haser S., 1992, A&A in press
Hodge P., 1989, ARA&A 27, 139
Husfeld D., Kudritzki R.P., Simon K.P., Clegg R.E.S., 1984, A&A 134, 139
Kaler J.B., Jacoby G.H., 1991, ApJ 372, 215
Kudritzki R.P., Hummer D.G., 1986, in: de Loore C.W., Willis A.J., Laskarides D. (eds.) Proc. IAU Symp. 116, Luminous Stars and Associations in Galaxies. Reidel, p.3
Kudritzki R.P., Hummer D.G., 1990, ARA&A 28, 303
Kudritzki R.P., Gabler R., Kunze D., Pauldrach A., Puls J., 1991, in: Leitherer C. et al. (eds.) Massive Stars in Starbursts. Cambridge Univ. Press, p.59
Kudritzki R.P., Hummer D.G., Pauldrach A., Puls J., Najarro F., Imhoff J., 1992, A&A in press
Méndez R.H., Kudritzki R.P., Herrero A., 1992, A&A in press
Osterbrock D.E., 1974, Astrophysics of Gaseous Nebulae. W.H. Freeman and Co., San Francisco, Table 2.8, p.35
Pakull M.W., Angebault L.P., 1986, Nature 322, 511
Pakull M.W., Motch C., 1989, Nature 337, 337
Pauldrach A., Puls J., Kudritzki R.P., Méndez R.H., Heap S.R., 1988, A&A 207, 123
Simon K.P., Jonas G., Kudritzki R.P., Rahe J., 1983, A&A 125, 34
Stasińska G., Testor G., Heydari-Malayeri M., 1986, A&A 170, L4
Vílchez J.M., Pagel B.E.J., 1988, MNRAS 231, 257
Walborn N.R., 1982, ApJ 254, L15

This article was processed by the author using Springer-Verlag LaTeX A&A style file 1990.